III European Conference on Computational Mechanics
Solids, Structures and Coupled Problems in Engineering
C.A. Mota Soares et.al. (eds.)
Lisbon, Portugal, 5–8 June 2006

NON-CONFORMING COUPLED TIME-DOMAIN BOUNDARY ELEMENT ANALYSIS

Martin Schanz[1] **and Thomas Rüberg**[2]

[1]Institute of Applied Mechanics
Graz University of Technology, Austria
m.schanz@tugraz.at

[2]Insititute of Structural Analysis
Graz University of Technology, Austria
rueberg@tugraz.at

Keywords: Time-Domain Boundary Element Analysis, Domain Decomposition, Soil-Structure Interaction

Abstract. *The time-domain Boundary Element Method has been found to be well suited for modeling wave propagation phenomena in large or unbounded media. Nevertheless, material discontinuities or local non-linear effects are beyond the scope of classical BEM and require special techniques. Here, a (possibly hybrid) Domain Decomposition method is proposed in order to circumvent these limitations.*

By means of local Dirichlet-to-Neumann maps and a weak statement of the interface conditions one obtains a concise formulation describing the global problem in a variational principle without specification of the descritization method (e.g., BEM or FEM).

Whereas this methodology has been fully established for elliptic partial differential equations, the aim is to transfer it to hyperbolic initial boundary value problems.

1 INTRODUCTION

Contrary to the popular belief that boundary element methods (BEM) compete with finite element methods (FEM), both methods are rather complementary [10]. Especially, in the case of the dynamic analysis of soil-structure interaction this fact becomes clear. The FEM is very well suited for the treatment of non-linear material behaviour in domains of finite size. Therefore, it is reasonable to discretise the structure and a surrounding box of soil where non-linearities are likely to occur with finite elements. On the other hand, the BEM is ill-suited for such non-linearities but very powerful for domains of large or infinite size. Moreover, it implicitly fulfils the radiation condition whereas a standard finite element discretisation yields artificial wave reflections polluting the numerical results in the given case.

Therefore, for the numerical analysis of the described and many other problems, such as, e.g., sound emission and fluid-structure interaction [3, 7], it is logical to make use of both methods, thus benefiting from the respective advantages.

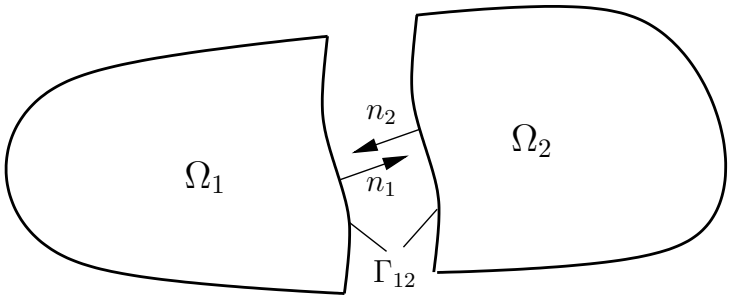

Figure 1: Domain Ω subdivided in two sub-domains, Ω_1 and Ω_2.

The standard approach to combine these methods is based on a *strong* fulfilment of the interface conditions, implying that the continuity requirement for the primal variable u (e.g., the pressure or the displacements) and the equilibrium condition for the dual variable q (e.g., the normal flux or the traction),

$$u|_{\Omega_1} = u|_{\Omega_2} \quad \text{and} \quad q|_{\Omega_1} + q|_{\Omega_2} = 0 \quad x \in \Gamma_{12}\,, \tag{1}$$

have to hold at every discretisation point on the interface Γ_{12} of the two sub-domains Ω_1 and Ω_2, see figure 1. This classical way to impose the interface conditions (1) is based on *conforming* discretisations at the interface, i.e., the discretisations of the sub-domains have to be such that their interface nodes coincide. This imposes a restriction which can simply cause practical inconveniences for the mesh generation, especially in case of the analysis of large structures with complicated geometries. But it can also conflict with stability conditions, especially in dynamic analyses (cf. Courant-Friedrichs-Lévy condition), when combining two different discretisation schemes.

In order to circumvent the latter problem, a coupling algorithm for the dynamic analysis of partitioned problems with boundary and finite element methods is proposed which is based on the incorporation of the interface conditions (1) in a *weak* form.

Within the context of finite element analysis of elliptic problems such methodology is well-established. Especially the so-called *mortar* element method has gained fame within the mathematical community (see the monograph of Wohlmuth [9] and references therein). Steinbach has put this method in a broader context and formulated method-independent *Dirichlet-to-Neumann*

maps, which allow for a concise theoretical analysis and the flexible use of both boundary and finite elements. Among other, his monograph [8] was an indispensable basis for this work.

Engineering applications of these ideas can be found for instance in [3] and [5]. In the former the classical mortar formulation with *global* Lagrange multipliers is used, whereas in the latter a three-field method is applied, whose theoretical background can be found in [8] as well.

2 A BOUNDARY-BASED FORMULATION FOR ELLIPTIC PROBLEMS

An elliptic boundary value problem can be given in the form

$$\begin{aligned} \mathcal{L}\,u(x) &= f(x) \quad x \in \Omega \\ u(x) &= \bar{u}(x) \quad x \in \Gamma_D \\ q(x) := \mathcal{T}(x)\,u(x) &= \bar{q}(x) \quad x \in \Gamma_N \end{aligned} \tag{2}$$

with the given Dirichlet and Neumann boundary values $\bar{u}$ and $\bar{q}$ on the respective boundary parts Γ_D and Γ_N. $\mathcal{L}$ is the elliptic differential operator of the problem (e.g., $\mathcal{L} = \Delta + \lambda$ for the Helmholtz equation) and $\mathcal{T}$ defines the co-normal derivative of u, which is the traction operator in elasticity.

A method-independent formulation motivates the boundary-based formulation of (2)

$$q(x) = \mathcal{S}(x)u(x) - \mathcal{N}(x)f(x) \quad x \in \Gamma\,, \tag{3}$$

which acts as a Dirichlet-to-Neumann map. The new operators are the Steklov-Poincaré operator $\mathcal{S}$ and the Newton potential $\mathcal{N}$ [8]. Together with the boundary conditions of (2), this formulation can be considered as an alternative representation to the given boundary value problem (2). A corresponding variational form is given by

$$\begin{aligned} \int_\Gamma (\mathcal{S}u)\,v\,\mathrm{d}s - \int_{\Gamma_D} q\,v\,\mathrm{d}s &= \int_{\Gamma_N} \bar{q}\,v\,\mathrm{d}s + \int_\Gamma (\mathcal{N}f)\,v\,\mathrm{d}s \\ \int_{\Gamma_D} u\,p\,\mathrm{d}s &= \int_{\Gamma_D} \bar{u}\,p\,\mathrm{d}s \end{aligned} \tag{4}$$

with weight functions v and p corresponding to u and q, respectively. Note, that the argument x has been omitted for the sake of a simpler notation. Effectively, the first equation of (4) states in a weighted form that the dual function q, obtained by the mapping (3), has to equal to the given $\bar{q}$ on the Neumann boundary Γ_N and to the unknown data of q on the Dirichlet boundary Γ_D. The second equation of (4) simply assures the weak fulfilment of the Dirichlet boundary conditions. In order to show the feasibility of this expression, it will be given in discrete form in the following. First, discretised with FEM and afterwards with BEM.

In classical FEM, a Galerkin approximation of the bilinear form appearing in the weak form of (2) yields a linear system of equations of the form $\mathbf{A}\mathbf{u} = \mathbf{f}$ with the stiffness matrix $\mathbf{A}$, the vector of nodal unknowns $\mathbf{u}$, and the force vector $\mathbf{f}$. Sorting the equations according to nodes in the interior of the domain and nodes on its boundary results in the block structured system

$$\begin{bmatrix} \mathbf{A}_{II} & \mathbf{A}_{\Gamma I} \\ \mathbf{A}_{I\Gamma} & \mathbf{A}_{\Gamma\Gamma} \end{bmatrix} \begin{bmatrix} \mathbf{u}_I \\ \mathbf{u}_\Gamma \end{bmatrix} = \begin{bmatrix} \mathbf{f}_I \\ \mathbf{f}_\Gamma \end{bmatrix}\,. \tag{5}$$

The indices $()_I$ and $()_\Gamma$ refer to the interior and the boundary of the domain and are only used in the finite element context and are otherwise omitted. Solving the first block system for the

unknowns $\mathbf{u}_I$ and inserting the result into the second equation yields the Schur-complement system

$$\underbrace{\left[\mathbf{A}_{\Gamma\Gamma} - \mathbf{A}_{\Gamma I}^T \mathbf{A}_{II}^{-1} \mathbf{A}_{I\Gamma}\right]}_{\mathbf{S}^{FEM}} \mathbf{u}_\Gamma = \mathbf{f}_\Gamma - \mathbf{A}_{\Gamma I}^T \mathbf{A}_{II}^{-1} \mathbf{f}_I \,. \tag{6}$$

The left hand side matrix is the FEM-discretisation of the operator $\mathcal{S}$ from the Dirichlet-to-Neumann map (3).

In BEM, a system of equations is obtained for the homogeneous problem, i.e., $f = 0$ in (2),

$$\left(\frac{1}{2}\mathbf{I} + \mathbf{K}\right) \mathbf{u} = \mathbf{V}\mathbf{q} \tag{7}$$

with the discretised single layer potential $\mathbf{V}$, double layer potential $\mathbf{K}$, the discrete identity $\mathbf{I}$, and the vectors of nodal unknowns for the primal and dual variables on the boundary, $\mathbf{u}$ and $\mathbf{q}$, respectively. The system matrices can be obtained from either the collocation or the Galerkin method as the underlying discretisation scheme. Here, only the first integral equation has been used. Now, a discrete Dirichlet-to-Neumann map can be easily established by

$$\underbrace{\mathbf{B}\mathbf{V}^{-1}\left(\frac{1}{2}\mathbf{I} + \mathbf{K}\right)}_{\mathbf{S}^{BEM}} \mathbf{u} = \mathbf{B}\mathbf{q} = \mathbf{f} \,. \tag{8}$$

This new *mass* matrix $\mathbf{B}$ merely contains integrals over the products of the trial functions for the primal and the dual variables and thus coincides with the discrete identity $\mathbf{I}$ in case of the Galerkin method, i.e., $\mathbf{B}[i,j] = \int_\Gamma \varphi_i \, \psi_j \, \mathrm{d}s$ when φ_i is a trial function for u and ψ_j for q. Nevertheless, in a collocation scheme these two matrices are different, because then $\mathbf{I}$ is the evaluation of the trial functions for the primal variable at the collocation points, i.e., $\mathbf{I}[i,j] = \varphi_j(x_i^*)$.

Returning now to the variational formulation (4), its discrete version can be written as the system of equations

$$\begin{bmatrix} \mathbf{S} & -\mathbf{B}_D \\ \mathbf{B}_D^T & \mathbf{0} \end{bmatrix} \begin{bmatrix} \mathbf{u} \\ \mathbf{q}_D \end{bmatrix} = \begin{bmatrix} \mathbf{f}_N \\ \mathbf{f}_D \end{bmatrix} \,, \tag{9}$$

where $\mathbf{u}$ contains the nodal values of the unknown function u on the whole boundary and $\mathbf{q}_D$ the nodal values of the function q on the Dirichlet boundary. $\mathbf{B}_D$ has the same definition as $\mathbf{B}$ but with the range of integration only on the Dirichlet boundary Γ_D. Moreover, there is a $\mathbf{B}_N$, which is defined analogously, and defines $\mathbf{f}_N = \mathbf{B}_N \bar{\mathbf{q}}$. In the same manner $\mathbf{f}_D$ contains the Dirichlet boundary conditions $\bar{\mathbf{u}}$. The matrix block $\mathbf{S}$ is obtained from a FEM (6) or a BEM (8) discretisation. Note that in case of an inhomogeneous problem and a FEM discretisation, simply the terms appearing on the right hand side of (6) have to be added to the first block equation in (9).

The expressions for $\mathbf{S}^{FEM}$ (6) and $\mathbf{S}^{BEM}$ (8) contain the inverse of a matrix, but this inverse does not have to be computed directly. In the case of a FEM discretisation for instance, one would replace the subsystem of type as in (9) by

$$\begin{bmatrix} \mathbf{A}_{II} & \mathbf{A}_{\Gamma I} & \mathbf{0} \\ \mathbf{A}_{I\Gamma} & \mathbf{A}_{\Gamma\Gamma} & -\mathbf{B} \\ \mathbf{0} & \mathbf{B}^T & \mathbf{0} \end{bmatrix} \begin{bmatrix} \mathbf{u}_I \\ \mathbf{u}_\Gamma \\ \mathbf{q}_D \end{bmatrix} = \begin{bmatrix} \mathbf{f}_I \\ \mathbf{f}_\Gamma \\ \mathbf{f}_D \end{bmatrix} \tag{10}$$

and thereby circumventing the computation of the inverse of $\mathbf{A}_{II}$.

For a BEM discretisation, the according matrix system would be

$$\begin{bmatrix} -\mathbf{V} & \frac{1}{2}\tilde{\mathbf{M}} & \mathbf{0} \\ \mathbf{M} & \mathbf{0} & -\mathbf{B} \\ \mathbf{0} & \mathbf{B}^T & \mathbf{0} \end{bmatrix} \begin{bmatrix} \mathbf{q} \\ \mathbf{u} \\ \mathbf{q}_D \end{bmatrix} = \begin{bmatrix} \mathbf{0} \\ \mathbf{f}_N \\ \mathbf{f}_D \end{bmatrix} \tag{11}$$

and the inverse of $\mathbf{V}$ must not be computed.

3 DOMAIN DECOMPOSITION FOR ELLIPTIC PROBLEMS

Now, consider the case of two sub-domains Ω_1 and Ω_2 with common interface Γ_{12} (see figure 1). In each sub-domain a boundary value problem of type (2) is defined, where the operators $\mathcal{L}_1$ and $\mathcal{L}_2$ need not be equal, and is complemented with the interface conditions (1). A consistent extension of the above boundary-based formulation (4) to a two-domain problem is

$$\begin{aligned}
\int_{\Gamma^1} (\mathcal{S}_1 u_1) v_1 \,\mathrm{d}s - \int_{\Gamma^1_D} q_1 \, v_1 \,\mathrm{d}s - \int_{\Gamma_{12}} \lambda (v_1 - v_2) \,\mathrm{d}s &= \int_{\Gamma^1_N} \bar{q}_1 \, v_1 \,\mathrm{d}s + \int_{\Gamma^1} (\mathcal{N}_1 f_1) v_1 \,\mathrm{d}s \\
\int_{\Gamma^2} (\mathcal{S}_2 u_2) v_2 \,\mathrm{d}s - \int_{\Gamma^2_D} q_2 \, v_2 \,\mathrm{d}s + \int_{\Gamma_{12}} \lambda (v_1 - v_2) \,\mathrm{d}s &= \int_{\Gamma^2_N} \bar{q}_2 \, v_2 \,\mathrm{d}s + \int_{\Gamma^2} (\mathcal{N}_2 f_2) v_2 \,\mathrm{d}s \\
\int_{\Gamma^1_D} u_1 \, p_1 \,\mathrm{d}s + \int_{\Gamma_{12}} (u_1 - u_2) \mu \,\mathrm{d}s &= \int_{\Gamma^1_D} \bar{u}_1 \, p_1 \,\mathrm{d}s \\
\int_{\Gamma^2_D} u_2 \, p_2 \,\mathrm{d}s - \int_{\Gamma_{12}} (u_1 - u_2) \mu \,\mathrm{d}s &= \int_{\Gamma^2_D} \bar{u}_2 \, p_2 \,\mathrm{d}s
\end{aligned} \tag{12}$$

with weight functions v_i and p_i (cf. [8] for a deeper insight concerning the specific trial spaces to be chosen). The interface conditions have been incorporated in a weak form by means of a Lagrange multiplier function λ with corresponding weight function μ. Actually, the Lagrange multiplier λ is physically the same as the dual function q. Here, it holds that $\lambda = q_1|_{\Gamma_{12}} = -q_2|_{\Gamma_{12}}$ (consequently, $\mu = p_1|_{\Gamma_{12}} = -p_2|_{\Gamma_{12}}$) and therefore the second of the interface conditions is prescribed in the classical strong form. Discretisation of the variational problem (12) yields the system of equations

$$\begin{bmatrix} \mathbf{S}_1 & \mathbf{0} & -\mathbf{B}_1 & \mathbf{0} & -\mathbf{C}_1 \\ \mathbf{0} & \mathbf{S}_2 & \mathbf{0} & -\mathbf{B}_2 & \mathbf{C}_2 \\ \mathbf{B}_1^T & \mathbf{0} & \mathbf{0} & \mathbf{0} & \mathbf{0} \\ \mathbf{0} & \mathbf{B}_2^T & \mathbf{0} & \mathbf{0} & \mathbf{0} \\ \mathbf{C}_1^T & -\mathbf{C}_2^T & \mathbf{0} & \mathbf{0} & \mathbf{0} \end{bmatrix} \begin{bmatrix} \mathbf{u}_1 \\ \mathbf{u}_2 \\ \mathbf{q}_{D1} \\ \mathbf{q}_{D2} \\ \boldsymbol{\lambda} \end{bmatrix} = \begin{bmatrix} \mathbf{f}_{N1} \\ \mathbf{f}_{N2} \\ \mathbf{f}_{D1} \\ \mathbf{f}_{D2} \\ \mathbf{0} \end{bmatrix} . \tag{13}$$

With this methodology, the interface meshes of the sub-domains do not have to match, since the continuity of u is not imposed point-wise. Nevertheless, the Lagrange multipliers inherit their mesh from one side, the *slave* side, using the terminology of the mortar element method [9], which is here Ω_1. Therefore, the computation of the entries of $\mathbf{C}_2$ requires integration over the interface of the product of the trial functions for λ and u_2, which do not necessarily live on the same mesh.

4 FINITE AND BOUNDARY ELEMENT METHODS FOR HYPERBOLIC PROBLEMS

An abstract hyperbolic boundary value problem has the form

$$\frac{\partial^2}{\partial t^2} u(x,t) - \mathcal{L}(x) u(x,t) = f(x,t) \quad x \in \Omega, \quad t \in (0,T)\,, \tag{14}$$

where $(0,T)$ is the interval on the time axis to be considered and $\mathcal{L}$ an elliptic differential operator. Furthermore, one needs the boundary conditions

$$\begin{aligned} u(x,t) &= \bar{u}(x,t) \quad x \in \Gamma_D, \quad t \in (0,T) \\ q(x,t) &= \bar{q}(x,t) \quad x \in \Gamma_N, \quad t \in (0,T) \end{aligned} \tag{15}$$

and the initial conditions

$$\begin{aligned} u(x,t) &= u_0(x) \quad x \in \Omega, \quad t = 0 \\ \frac{\partial}{\partial t} u(x,t) &= v_0(x) \quad x \in \Omega, \quad t = 0 \end{aligned} \tag{16}$$

to completely describe the problem. Classical examples for equations of type (14) are the scalar wave equation and the elastodynamic equations.

The classical FEM approach to these equations is to perform the spatial discretisation as in the elliptic case and obtain the semi-discrete system of equations [4]

$$\mathbf{M}\ddot{\mathbf{u}}(t) + \mathbf{A}\mathbf{u}(t) = \mathbf{f}(t) \tag{17}$$

with the mass and stiffness matrices, $\mathbf{M}$ and $\mathbf{A}$, respectively. Application of Newmark's method for time discretisation yields the solution after $n+1$ time steps of size h in the form

$$\begin{aligned} \left[\mathbf{M} + h^2\beta\mathbf{A}\right]\mathbf{u_{n+1}} = &\left[2\mathbf{M} - h^2\left(\frac{1}{2} - 2\beta + \gamma\right)\mathbf{A}\right]\mathbf{u}_n \\ &- \left[\mathbf{M} - h^2\left(\frac{1}{2} + \beta - \gamma\right)\mathbf{A}\right]\mathbf{u}_{n-1} \\ &+ h^2\left[\beta\mathbf{f}_{n+1} + \left(\frac{1}{2} - 2\beta + \gamma\right)\mathbf{f}_n + \left(\frac{1}{2} + \beta - \gamma\right)\mathbf{f}_{n-1}\right] \end{aligned} \tag{18}$$

with the method-specific parameters β and γ [4]. The system (18) can be abbreviated as

$$\mathbf{A}_0\mathbf{u}_{n+1} = \mathbf{A}_1\mathbf{u}_n + \mathbf{A}_2\mathbf{u}_{n-1} + \mathbf{f}_{n+1}\,. \tag{19}$$

Reordering these equations as it has been done in (5), one can obtain similarly to (6)

$$\tilde{\mathbf{S}}^{FEM}\mathbf{u}_{n+1,\Gamma} = \tilde{\mathbf{f}}_{n+1} \tag{20}$$

which provides a discrete Dirichlet-to-Neumann map for the current time step. Note, that in the given case the left hand side matrix does not change throughout the computation if an equidistant time grid is chosen.

In the case of BEM, one gets for the homogeneous equation with vanishing initial conditions, i.e., $f = u_0 = v_0 = 0$, in operator form [2]

$$\left(\frac{1}{2}\mathcal{I} + \mathcal{K}\right) * u = \mathcal{V} * q \tag{21}$$

where $*$ denotes the time convolution, i.e., $g * h = \int_0^t g(\tau - t)h(\tau)\,\mathrm{d}\tau$. The operators are the identity $\mathcal{I}$, the single layer $\mathcal{V}$ and the double layer $\mathcal{K}$ potential. Choosing a certain time

discretisation, e.g., the convolution quadrature method or analytical time integration [6], one obtains the recursive system of equations

$$\left(\frac{1}{2}\mathbf{I}+\mathbf{K}_0\right)\mathbf{u}_{n+1}+\sum_{i=1}^{n}\mathbf{K}_{n-i}\mathbf{u}_i=\mathbf{V}_0\,\mathbf{q}_{n+1}+\sum_{i=1}^{n}\mathbf{V}_{n-i}\mathbf{q}_i \tag{22}$$

which, in the same manner as in (8), can be reformulated to

$$\underbrace{\mathbf{B}\,\mathbf{V}_0^{-1}\left(\frac{1}{2}\mathbf{I}+\mathbf{K}_0\right)}_{\tilde{\mathbf{S}}^{BEM}}\mathbf{u}_{n+1}=\mathbf{B}\,\mathbf{q}_{n+1}+\mathbf{B}\,\mathbf{V}_0^{-1}\sum_{i=1}^{n}\left(\mathbf{V}_{n-i}\mathbf{q}_i-\mathbf{K}_{n-i}\mathbf{u}_i\right)=\tilde{\mathbf{f}}_{n+1}\,. \tag{23}$$

Similarly to the elliptic case, the discrete Dirichlet-to-Neumann map for the current time step, as given in (20) or (23), can now be replaced by either its FEM or its BEM discretisation. Moreover, the same replacement of subsystems as in (10) and (11), respectively, can be carried out to avoid the computation of an inverse matrix.

Be means of (20) and (23), discrete mappings from the primal to the dual variable on the boundary, i.e., from $\mathbf{u}$ to $\mathbf{q}$, have been established. Therefore, by keeping the time step fixed the discrete system of equations for a coupled problem (13) as derived in section 3 can be reused for the hyperbolic problem.

5 EXAMPLE

As a test example, the homogeneous scalar wave equation is considered

$$\frac{\partial^2}{\partial t^2}u(x,t)-c^2\Delta u(x,t)=0 \tag{24}$$

where c denotes the wave velocity. Initial conditions are assumed to be identical zero. The considered two-dimensional domain is $\Omega=(0,2)\times(0,1)$ which will be subdivided into two squares, $\Omega_1=(0,1)\times(0,1)$ and $\Omega_2=(1,2)\times(0,1)$, see figure 2. In this specific problem, the primal variable u can be considered the fluid pressure and the dual variable q the normal flux at the boundaries, $q=\frac{\partial}{\partial\mathbf{n}}u$ with the outward normal vector $\mathbf{n}$.

In the computation, zero Dirichlet boundary conditions are prescribed, $\bar{u}=0$, on the boundary part Γ_1 (cf. figure 2, right). A unit step function $\bar{q}(t)=H(t)$ is applied on the side Γ_3 and zero Neumann conditions, $\bar{q}=0$, elsewhere. The wave velocities are assumed to be equal in both sub-domains, i.e., $c_1=c_2=1$. For the FEM discretisation, 10×10 bi-linear quadrilaterals have been used for Ω_1 and 9×9 for Ω_2. The BEM computation has been carried out with 10 linear elements in the first sub-domain and 9 linear elements for the second. These numbers were chosen arbitrarily to ensure non-conforming interface meshes. Figure 2 shows the FEM and BEM meshes and it can be seen that the interface mesh is inherited from Ω_1, the so-called slave side. The Lagrange multipliers λ and normal fluxes q are assumed to be linear as well but discontinuous at the corners. The discretisations are depicted in figure 2, on the right.

Figure 2, left, shows the results for a coupled FEM (top) and a coupled BEM (bottom) computation for the given problem and the first 20 time units. The chosen time steps are $h_{FEM}=0.005$ for the finite element and $h_{BEM}=0.05$ for the boundary element discretisation.

This example has been chosen merely to show the feasibility of the proposed method. The numerical results show a fairly good agreement with the analytical solution.

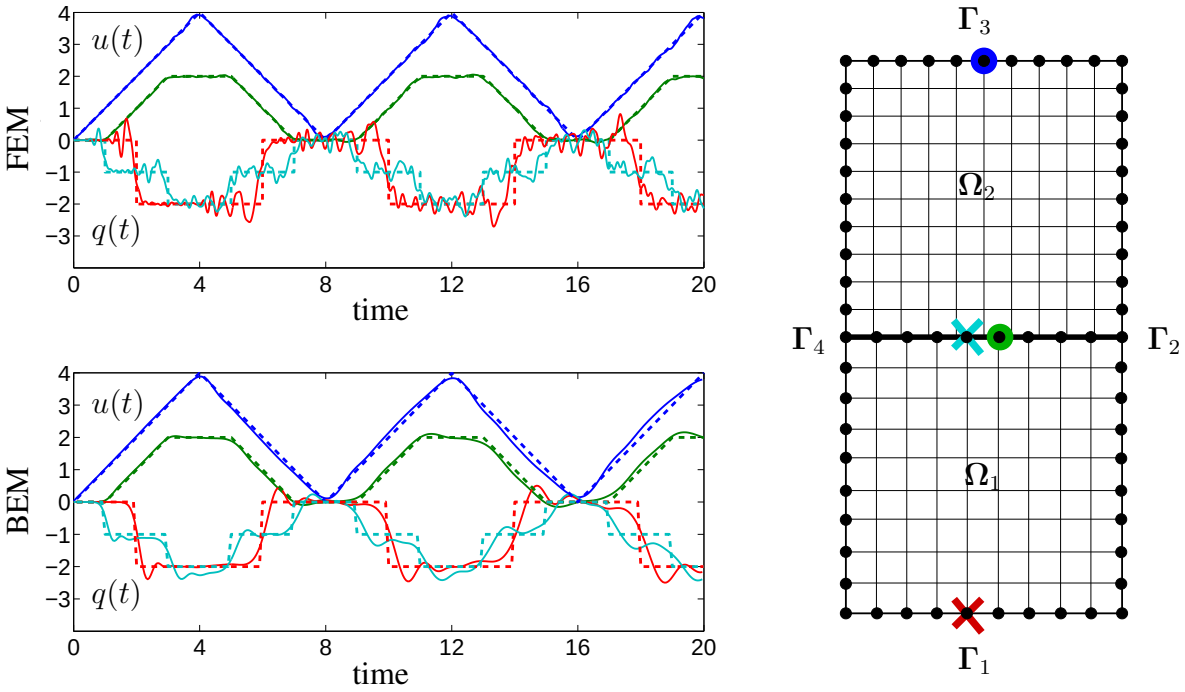

Figure 2: Problem description (right) with points of evaluation (circles for u, crosses for q) and the chosen FEM mesh and boundary elements. The top picture shows the results of a finite element and the bottom picture the results of boundary element analysis. The computed solution is shown by solid lines and the analytical solution by dashed lines. The zig-zag curves represent the pressure $u(t)$ at the side of the applied unit step function (blue) and the interface (green). The piece-wise constant curves represent the normal flux $q(t)$ at the interface (cyan) and at the Dirichlet boundary (red).

A second simulation was performed by changing the wave velocity in sub-domain Ω_2 to $c_2 = 2$. Due to the lack of an analytical solution, in figure 3 simply the results of the numerical solution are shown. This computation has been only carried out with a BEM discretisation and could not have been performed with a single-domain approach, since there does not exist a fundamental solution for discontinuous material parameters.

Contrary to the first test with equal wave velocities in both domains, the interpretation of the results is not as easy as before. In the first example in figure 2, the primal variable at the free end Γ_3 (depicted in blue) shows clearly the wave reflections, e.g., after four time units the

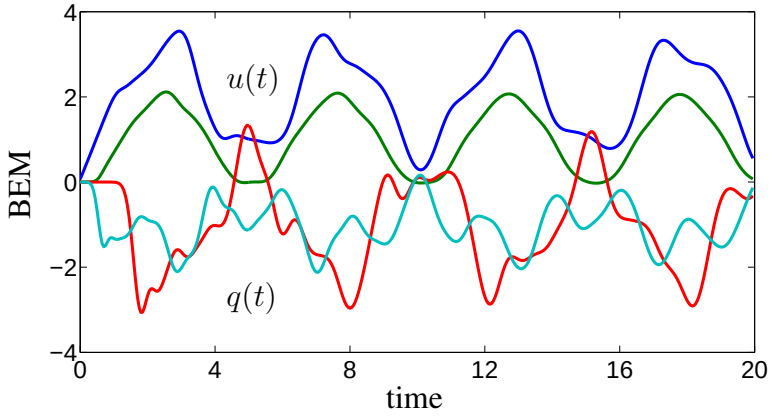

Figure 3: Solution curves for the case of $c_2 = 2$ and $c_1 = 1$. The colours refer to the same points as in figure 2.

wave front has travelled to the bottom and back. Then, it is reflected at the free end causing a reduction of the value of $u(t)$. This reflection can be observed also for later times resulting in a periodic figure. Here, in the second example, the various reflections can not been traced because, now, there are reflections at the interface Γ_{12} and at the fixed end at Γ_1. However, some wave phenomena can be identified in figure 3. The slope at the beginning of the blue line in figure 3 corresponds to the wave velocity $c_2 = 2$ in domain Ω_2 until the first wave reflection at the interface is observed at time unit one. Then, the slope is decreased to one corresponding to the wave velocity $c_1 = 1$ in domain Ω_1. The next slight change at time unit two should be the second reflection at the interface, however, as this is no longer a reflection at a fixed end it is no sharp change. The kink at time unit three may be interpreted as the arrival of a wave reflected at the bottom Γ_1, i.e., the wave propagated from top to the bottom and back to the top. More reflections can not be clearly identified, but due to these first identifiable wave reflections the results seem to be reasonable.

6 CONCLUSION

By comparison of a well-established formulation of non-conforming domain decomposition for elliptic problems (mainly based on [8]) with the discrete equations arising in the treatment of hyperbolic problems with either the finite or the boundary element method, an algorithm for the treatment of coupled time-domain problems with non-matching interface meshes has been proposed. Small test examples show the feasibility of this method.

Nevertheless, the efficient solution of the final systems of equations has yet to be formulated. Especially, the fact, that the system matrices might not change throughout the time steps, leads to the question whether an iterative solver can still be more efficient than a direct solver. In the same context, data-sparse methods seem appealing for an efficient treatment of the fully populated BEM matrices [1].

Next to these numerical issues, the possible extension to multi-physical problems, where the local differential operators are not the same (fluid-structure interaction, sound emission [3], poro- and viscoelastic wave propagation [6], etc.), has to be analysed.

REFERENCES

[1] M. Bebendorf. *Adaptive Low-Rank Approximation of Collocation Matrices*. Computing, **74**, 225–47, 2005.

[2] M. Costabel. *Time-dependent problems with the boundary integral equation method*. E. Stein, R. de Borst, and T.J.R. Hughes eds. *Encyclopedia of Computational Mechanics*, Chapter 25, Volume 1. John Wiley & Sons, New York, 2004.

[3] M. Fischer and L. Gaul. *Fast BEM-FEM Mortar Coupling for Acoustic-Structure Interaction*. International Journal of Numerical Methods in Engineering, **62**, 1677–1690, 2005.

[4] T.J.R. Hughes. *The finite element method*. Prentice-Hall,Englewood Cliffs, New Jersey, 1987.

[5] K.C. Park, C.A. Felippa, and U.A. Gumaste. *A localized version of the method of Lagrange multipliers and its applications*. Computational Mechanics, **24**, 476–490, 2000.

[6] M. Schanz. *Wave Propagation in Viscoelastic and Poroelastic Continua*. Springer, Heidelberg, 2001.

[7] D. Soares Jr., O. von Estorff, and W.J. Mansur. *Iterative coupling of BEM and FEM for nonlinear dynamic analyses*. Computational Mechanics, **34**, 67–73, 2004.

[8] O. Steinbach. *Stability Estimates for Hybrid Domain Decomposition Methods*. Springer-Verlag, Heidelberg, 2003.

[9] B.I. Wohlmuth. *Discretization Methods and Iterative Solvers Based on Domain Decompostion*. Springer-Verlag, Heidelberg, 2001.

[10] O.C. Zienkiewicz, D.W. Kelly, and P. Bettess. *The coupling of the finite element method and boundary solution procedures*. International Journal of Numerical Methods in Engineering, **11**, 355–375, 1977.